Blood. Author manuscript; available in PMC 2010 June 24.

Published in final edited form as:
Blood. 2005 September 15; 106(6): 2189–2195. doi:10.1182/blood-2005-02-0629.

Contribution of *Hfe* expression in macrophages to the regulation of hepatic hepcidin levels and iron loading

Hortence Makui, **Ricardo J. Soares**, **Wenlei Jiang**, **Marco Constante**, and **Manuela M. Santos**

Centre de recherche, Centre hospitalier de l'Université de Montréal (CHUM)–Hôpital Notre-Dame, Montréal, Québec, Canada; and UnIGENe, Instituto de Biologia Molecular e Celular, Porto, Portugal

Abstract

Hereditary hemochromatosis (HH), an iron overload disease associated with mutations in the *HFE* gene, is characterized by increased intestinal iron absorption and consequent deposition of excess iron, primarily in the liver. Patients with HH and *Hfe*-deficient *($Hfe^{-/-}$)* mice manifest inappropriate expression of the iron absorption regulator hepcidin, a peptide hormone produced by the liver in response to iron loading. In this study, we investigated the contribution of *Hfe* expression in macrophages to the regulation of liver hepcidin levels and iron loading. We used bone marrow transplantation to generate wild-type (wt) and $Hfe^{-/-}$ mice chimeric for macrophage *Hfe* gene expression. Reconstitution of *Hfe*-deficient mice with wt bone marrow resulted in augmented capacity of the spleen to store iron and in significantly decreased liver iron loading, accompanied by a significant increase of hepatic hepcidin mRNA levels. Conversely, wt mice reconstituted with *Hfe*-deficient bone marrow had a diminished capacity to store iron in the spleen but no significant alterations of liver iron stores or hepcidin mRNA levels. Our results suggest that macrophage *Hfe* participates in the regulation of splenic and liver iron concentrations and liver hepcidin expression.

Introduction

Hereditary hemochromatosis (HH) type 1, an autosomal recessive disease of iron overload, is one of the most common inherited disorders. It is characterized by failure in the regulation of duodenal iron absorption, leading to iron overloading that can eventually impair organ systems and cause cirrhosis, diabetes, and cardiomyopathy.[1]

HH is caused by mutations in the *HFE* gene encoding a major histocompatibility complex (MHC) class 1–like protein that requires β2-microglobulin (B2m) for cell surface expression.[2] A link between HFE and cellular iron metabolism is suggested by the observation that wild-type (wt) HFE-β_2m molecules form a stable complex with transferrin receptor 1 (TfR1).[3]

Reprints: Manuela Santos, CHUM-Hôpital Notre-Dame, Pav. De Sève Y5625, 1560 Sherbrooke est, Montréal, Québec H2L 4M1, Canada; manuela.santos@umontreal.ca.

Most patients with HH are homozygous for a missense mutation in the *HFE* gene that results in cysteine-to-tyrosine substitution at amino acid 282 of HFE protein (C282Y).[2] The mutation disrupts a critical disulfide bond in the α_3 domain of HFE protein and abrogates binding of the mutant HFE protein to B2m, leading to impaired HFE protein intracellular trafficking, incorporation into the cell membrane, and association with TfR1.[3]

Studies in mice with targeted inactivation of the *Hfe* or *B2m* gene have confirmed the critical role of HFE-B2m complexes in iron metabolism.[4–6] As do humans with HH, Hfe-deficient mice develop iron overloading with an accumulation of excess iron, primarily in liver parenchymal cells, as opposed to reticuloendothelial (RE) cell storage characteristic of secondary iron overload. Thus, abnormal regulation of iron metabolism in RE cells seems to take place in HH because these cells are relatively iron deficient compared with surrounding parenchymal hepatocytes.[7] Importantly, RE cells—monocytes and tissue macrophages—have a central role in regulating iron homeostasis because they recognize and phagocytose senescent and damaged erythrocytes, process iron from heme, and return it to the circulation for reuse by red cell precursors during erythropoiesis.[8]

In a previous study, we showed that the reconstitution of $B2m^{-/-}$ mice with normal hematopoietic cells leads to cellular redistribution of iron stored in the liver,[6] suggesting an important role of *Hfe* expression in hematopoietic-derived cells in iron homeostasis. This was based on a histologic investigation into iron distribution in the liver. In this model, attempts to reconstitute wt-type mice with $B2m^{-/-}$ hematopoietic cells failed because of rejection of the transplanted MHC class 1–negative cells by host natural killer (NK) cells.[9]

There is now considerable evidence that *Hfe*-deficiency results in inappropriate expression of the putative iron regulator hepcidin in animal models[10,11] and in patients with HH.[12] Hepcidin, the product of the *Hamp* gene, is a β-defensin–like antimicrobial peptide[13] whose liver expression is modulated by iron stores, anemia/hypoxia, and inflammation.[14,15] Further convincing evidence of an essential role for hepcidin in iron metabolism and in the regulation of intestinal iron uptake is provided by findings that hepcidin knockout mice develop severe iron overload,[16] whereas, conversely, transgenic mice overexpressing hepcidin incur severe anemia.[17]

In the present study, we investigated the functional role of Hfe in macrophages and the contribution of this cell type to the regulation of liver hepcidin levels and iron loading by using bone marrow transplantation (BMT). We used the $Hfe^{-/-}$ mouse model for BMT to generate mice expressing *Hfe* in RE macrophages and mice with selected inactivation of *Hfe* in RE macrophages.

Materials and methods

Animals

All procedures were performed in accordance with Canadian Council on Animal Care guidelines after approval by the Institutional Animal Care Committee of the Centre hospitalier de l'Université de Montréal (CHUM). $Hfe^{-/-}$ mice were kindly provided by Dr Nancy C. Andrews (Howard Hughes Medical Institute and Harvard Medical School,

Children's Hospital, Boston, MA).[5] The *Hfe*$^{-/-}$ and wt mice in these experiments, females from the 129/SvEvTac background, were permanently housed under specific pathogen-free conditions. Green fluorescence protein (GFP) transgenic mice (GFP^{+}wt) expressing GFP from the chicken Actb promoter (strain Tg[Actb-EGFP]) were purchased from Jackson ImmunoResearch Laboratories (West Grove, PA) and were backcrossed 5 times with 129/SvEvTac mice in our animal facility. GFP^{+}*Hfe*$^{-/-}$ transgenic mice were obtained by crossing *Hfe*$^{-/-}$ mice with GFP^{+}wt mice.

Cell preparations

Spleens were mashed through a 40-μm nylon cell strainer, and erythrocytes in splenocyte suspensions were lysed with Puregene RBC Lysis Solution (Gentra Systems, Minneapolis, MN). Livers were perfused with liver digest media (Gibco/BRL Life Technologies, Burlington, ON, Canada), and the resultant suspension was centrifuged at 70*g* for 5 minutes to separate hepatocytes (pellet) and nonparenchymal cells (NPCs; supernatant). Mononuclear cells (MNCs) were obtained by centrifugation of NPC suspensions on Lympholyte-M (Cedarlane, Hornby, ON, Canada). B lymphocytes, T lymphocytes, NK cells, and macrophages were isolated from splenocyte and NPC suspensions by positive magnetic cell separation, with EasySep kits (Stem Cell Technologies, Vancouver, BC, Canada). The following antibodies (PharMingen, San Diego, CA) were used: CD45R/B220 (B cells), CD90/Thy-1 (T cells), panNK-PE (NK cells), and F4/80 (macrophages and Kupffer cells). Enrichment of the recovered B220^{+}, CD90^{+}, NK^{+}, and F4/80^{+} cells was confirmed by flow cytometric analysis (Coulter Epics Elite counter; Coulter, Hialeah, FL) and was routinely greater than 95%.

Bone marrow transplantation

Bone marrow cells were harvested by flushing the femurs and tibias of wt and *Hfe*$^{-/-}$ mice with medium. Six-week-old female wt mice and *Hfe*$^{-/-}$ mice were lethally irradiated (9.5 Gy) and served as recipients. Irradiated mice intravenously received 10 to 15 × 10^{6} bone marrow cells from wt or *Hfe*$^{-/-}$ mice and were killed 14 weeks after BMT. In experiments in which bone marrow cells were harvested from GFP^{+}wt and GFP^{+}*Hfe*$^{-/-}$ mice, wt or *Hfe*$^{-/-}$ mice that underwent transplantation were screened by flow cytometry for GFP^{+} leukocytes in the liver. B cells, T cells, and macrophages in nonparenchymal cells of the liver were identified by fluorescence-activated cell sorter (FACS) staining with anti-B220, anti–T-cell receptor (TCR), and anti-F4/80, respectively.

Quantitative and conventional reverse transcription–polymerase chain reaction

Total RNA was isolated with Trizol reagent (Invitrogen, Burlington, ON, Canada), and reverse transcription (RT) was performed with the Thermo-script RT-PCR system (Invitrogen). Levels of *Hfe*, Actb, hepcidin (*Hamp*), and glyceraldehyde-3-phosphate dehydrogenase (*Gapdh*) mRNA were measured by real-time PCR in a Rotor Gene 3000 Real Time DNA Detection System (Montreal Biotech Inc, Kirkland, QC, Canada) with the QuantiTect SYBRGreen I PCR kit (Qiagen, Mississauga, ON, Canada). All primers were designed with Primer3 software to include at least one intron. For each primer pair, the amplified cDNA fragments were verified in agarose gel to confirm the absence of the intron on the amplified fragment and the absence of nonspecific products. The primers used were:

wt-type Hfe *(wtHfe)*, 5′GAATGGGACGAGCACAAGAT3′ and 5′TGATGTTCTGGGGGAAGAAG3′; mutated Hfe *(neoHfe)*, AGTTGGGAGTGGTGTCCGA3′ and CTAGCTTCGGCCGTGACG; *Actb*, 5′-TGTTACCAACTGGGACGACA-3′ and 5′-GGTGTTGAAGGTCTCAAA-3′; *Hamp,* 5′AGAGCTGCAGCCTTTGCAC3′ and 5′GAAGATGCAGATGGGGAAGT3′; and *Gapdh,* 5′TCAAGAAGGTGGTGAAGCAG3′ and 5′TGGGAGTTGCTGTTGAAGTC3′. Relative quantitation was performed using standard curves constructed from serial dilutions of PCR products. All standard curves generated were found to have excellent PCR amplification efficiency (90%–96%; 100% indicates that after each cycle the amount of template is doubled), as determined by their slopes. mRNA expression for each gene was determined by direct comparison with the standard curve of the specific target generated in each PCR run. Expression levels were normalized to the housekeeping gene *Gapdh* or to *Actb*.

For conventional PCR used in *Hfe* expression studies, the primers were: *Hfe,* 5′AGTTGGGAGTGGTGTCCGA3′ and 5′CCTCCAAGTCTTTGGCTGAG3′; and *Actb,* 5′-AGCCATGTACGTAGCCATCC-3′ and 5′-TTTGATGTCACGCACGATTT-3′. Amplified RT-PCR products were visualized by ethidium bromide staining in 1.0% agarose gels.

Hematologic measurements and transferrin saturation

Red blood cell (RBC) count, hemoglobin (Hb) level, hematocrit (HCT), and mean corpuscular volume (MCV) were measured with an automated cell counter calibrated for murine samples (ABC *vet* counter; ABX hématologie, Montpellier, France). Serum iron, total iron-binding capacity (TIBC), and transferrin saturation were assessed by colorimetric assay[18] with the Kodak Ektachem DT60 system (Johnson & Johnson, Ortho-Clinical Diagnostics, Mississauga, ON, Canada).

Measurement of tissue iron concentration

Liver and spleen iron concentrations were assessed by acid digestion of tissue samples, followed by iron quantification with atomic absorption spectroscopy.[18]

Statistical analysis

All values in the figures are expressed as mean plus or minus SD. Student *t* test (unpaired, 2-tailed) was used for comparison between 2 groups. Multiple comparisons were statistically evaluated by one-way analysis of variance (ANOVA) followed by the Tukey test.

Results

qRT-PCR analysis of *Hfe* expression in various mouse organs and in isolated cell fractions

Previous reports using immunocytochemistry showed that human HFE protein is abundantly expressed in the small intestine, particularly in duodenal crypt cells,[19] whereas in the liver, HFE is found in Kupffer cells.[20] Recent studies with RT-PCR analysis, in situ hybridization, and Western blot analysis demonstrated HFE expression also in rat hepatocytes.21,22 We examined the pattern of *Hfe* expression in mice by quantitative RT-PCR (qRT-PCR). As

shown in Figure 1A, we found that the mouse *Hfe* gene is expressed in most organs, with the highest expression levels in the liver, heart, and skeletal muscle, followed by the kidneys, lungs, and spleen. The lowest mRNA levels were found in the duodenum, thymus, brain, and bone marrow. These results are consistent with previous work on the *Hfe* expression pattern in mice by Northern blot analysis.[23]

To determine which hematopoietic cell lineages express *Hfe*, we performed qRT-PCR analysis in purified splenic cell populations (Figure 1B). *Hfe* was highly expressed in macrophages ($F4/80^+$ cells) but was barely detectable in B and T lymphocytes or in NK cells.

Similarly, in the liver, macrophages expressed high *Hfe* mRNA levels, whereas considerably lower levels were observed in intrahepatic MNC isolates, which consisted mostly of T and B lymphocytes with 4% to 8% $F4/80^+$ cells.

Iron misregulation in *Hfe*$^{-/-}$ mice

The severity of iron overloading and the expression levels of liver hepcidin in HH animal models are known to depend on genetic background, age, and sex.[24–28] Thus, we assessed the degree of iron loading in 2 *Hfe*-deficient mouse strains, 129/SvEvTac and C57Bl/6, by measuring serum iron levels, transferrin saturation, and iron concentrations in the liver and spleen. We used qRT-PCR analysis to quantify hepatic *Hamp* mRNA levels in wt and *Hfe*$^{-/-}$ mice.

As expected, serum iron levels and transferrin saturation were significantly elevated in *Hfe*-deficient 10-week-old females from the 129/SvEvTac background (Table 1). Hepatic iron concentration was 5-fold higher in *Hfe*$^{-/-}$ mice, whereas splenic iron levels were not significantly different from those of wt mice (Table 1). Resistance to iron loading in the spleens of *Hfe*-deficient mice has been observed previously[4,29] and is believed to be caused by defective handling of iron in macrophages.

A 6-fold reduction of hepatic *Hamp* mRNA expression was detected in *Hfe*$^{-/-}$ compared with wt mice (Figure 2). These results are consistent with previously reported data[11] and with the scenario that the lack of *Hfe* expression leads to inappropriate hepatic *Hamp* levels and ultimately to augmented duodenal iron absorption in this Hfe-deficient mouse strain. When similar studies were performed in *Hfe*-deficient mice of the same age and sex that had been backcrossed 11 times onto the C57Bl/6 background, the degree of iron loading was significantly lower (1675 ± 249 μg in 129/SvEvTac vs 739 ± 228 μg iron/g dry weight in C57Bl/6; $P < .001$; n = 6 per group). In addition, hepatic *Hamp* mRNA levels, albeit lower, were not significantly different from those found in wt C57Bl/6 mice (data not shown).

Based on our data and to monitor the effects of BMT on iron homeostasis, we tested *Hfe*-deficient mice from the 129/SvEvTac background in subsequent studies.

BMT studies

To investigate the importance of *Hfe* expression on RE macrophages in the regulation of iron homeostasis, we transplanted bone marrow from wt mice into lethally irradiated *Hfe*$^{-/-}$ mice

to obtain mice that expressed *Hfe* in macrophages. Furthermore, we generated mice lacking *Hfe* expression in macrophages, but not in hepatocytes or in intestinal epithelial cells, by transplanting bone marrow from $Hfe^{-/-}$ mice into wt recipients. To control for the effects of irradiation, respective controls were generated by wt → wt and $Hfe^{-/-}$ → $Hfe^{-/-}$ transplantations.

Given that earlier BMT studies show that bone marrow cells (BMCs) have the potential to differentiate into various cell types in the liver, including hepatocytes[30,31] and Kupffer cells,[32] we first set out to evaluate the cell fate potential of transplanted BMCs in the liver using a cell-marking method with GFP transgenic mice. To generate a source of $GFP^{+}Hfe^{-/-}$ BMCs, we crossed *Hfe* mutant mice with transgenic animals that constitutively express GFP in all tissues under control of the chicken *Actb* promoter.[33] Chimeric animals were produced by transplantation of $GFP^{+}Hfe^{-/-}$ or GFP^{+}wt BMCs into GFP-negative, wt, or $Hfe^{-/-}$ irradiated recipients. Nonparenchymal cells from the liver were isolated and analyzed by flow cytometry to determine the degree of reconstitution in animals after transplantation, as described in "Materials and methods." We found that approximately 33% to 37% of liver macrophages, identified as cells expressing the macrophage-specific marker F4/80, were of donor origin (ie, GFP positive), whereas 63% to 67% of total macrophages were of host origin because they were negative for GFP expression (Table 2). No significant differences were observed between the different BMT groups, indicating that $Hfe^{-/-}$ BMCs have a capacity similar to that of wt BMCs to repopulate irradiated recipients.

To evaluate the potential of transplanted BMCs to generate hepatocytes, we analyzed liver tissues from engrafted recipients for the presence of GFP^{+} hepatocytes (GFP^{+}, albumin-positive cells) by fluorescence microscopy. No GFP^{+} hepatocytes were detected in any of the recipient mice (data not shown).

These results demonstrate that wt and $Hfe^{-/-}$ BMCs can reconstitute approximately one third of liver macrophages but that BMCs contribute little or not at all to the replacement of hepatocytes in the context of iron overload caused by Hfe deficiency. This is in agreement with a number of more recent studies using several models and showing that, under physiologic conditions and without the presence of strong selection pressure, bone marrow–derived hepatocytes are rarely, if at all, generated[34–37] (for a review, see Fausto[38]).

Successful engraftment of donor bone marrow cells after 14 weeks was also assessed by conventional RT-PCR analysis of *Hfe* mRNA from total liver, spleen, and duodenal extracts using primers that span exon 3 to exon 6 of the *Hfe* gene. Amplification of cDNA obtained from wt and $Hfe^{-/-}$ mice yielded 775-bp and approximately 499-bp products, respectively (Figure 3), because of the deletion of the entire exon 4 (approximately 276 bp) in $Hfe^{-/-}$ mice.[29] Expression of disrupted, exon 4–deficient *Hfe* mRNA was detected in the total liver, spleen, and duodenum of wt mice repopulated with $Hfe^{-/-}$ bone marrow, but not in those that underwent transplantation with control wt bone marrow (Figure 3). The opposite (ie, intact *Hfe* mRNA) was detected in samples from $Hfe^{-/-}$ mice repopulated with wt bone marrow.

To further quantify donor mRNA in *Hfe*$^{-/-}$ → wt and wt → *Hfe*$^{-/-}$ mice, we used qRT-PCR (Figure 3). wt and mutant *Hfe* were separately amplified with primers *wtHfe* and *neoHfe*, as described in "Materials and methods." In the liver, donor mRNA was approximately 7% to 8% of the level observed in the relevant BMT control group (Figure 3A). Because Kupffer cells represent approximately 20% of the liver, these results suggest approximately 35% to 40% repopulation of liver macrophages from the donor marrow, assuming that *Hfe* expression in donor macrophages is similar to that in host macrophages. In the spleen, 92% to 95% of mRNA detected in BMT chimeras was of donor origin (Figure 3B).

Overall, engraftment efficiency in our BMT mice was similar to that reported in other studies, which found 20% to 35% replacement of macrophages in the liver 8 weeks after BMT and 80% to 95% replacement of plasma leukocytes 4 to 5 weeks after BMT.[39–42] In the duodenum, donor mRNA reached 34% to 36% of the levels encountered in the pertinent BMT control group (Figure 3C).

Given that *Hfe* is highly expressed in macrophages compared with lymphocytes (Figure 1B–C), these findings are consistent with the accumulation of bone marrow–derived wt macrophages in the liver, spleen, and duodenum of wt → *Hfe*$^{-/-}$ mice and of *Hfe*-deficient macrophages in *Hfe*$^{-/-}$ → wt mice.

Serum iron and transferrin saturation analysis

Next, we examined changes in serum iron (SI) levels and transferrin saturation (TS), the earliest laboratory abnormalities in HH. SI and TS were significantly higher in *Hfe*$^{-/-}$ → *Hfe*$^{-/-}$ mice than in wt → wt mice (SI, 50 ± 3 μM vs 25 ± 5 μM, respectively; TS, 115% ± 8% vs 58% ± %15, respectively; $P < .001$), as expected,[29] and were not affected by changes of *Hfe* expression in macrophages in BMT chimeras (data not shown).

Alterations of iron levels in bone marrow chimeras

To monitor changes in body iron levels in BMT mice, we measured its concentration and calculated total iron in livers and spleens, the most relevant organs of iron storage. We found that wt mice whose bone marrow had been reconstituted with *Hfe*-deficient cells (*Hfe*$^{-/-}$ → wt) did not have significantly altered iron concentrations in the liver. In contrast, *Hfe*$^{-/-}$ mice reconstituted with wt cells (wt → *Hfe*$^{-/-}$) had significantly decreased iron concentrations in the livers compared with control *Hfe*$^{-/-}$ → *Hfe*$^{-/-}$ mice (1920 ± 477 μg vs 2774 ± 380 μg iron/g dry weight, respectively) (Figure 4A).

Surprisingly, splenic iron concentrations were reduced by 38% in *Hfe*$^{-/-}$ → wt mice (Figure 4B). In fact, the capacity to store iron in the spleen was significantly impaired in *Hfe*$^{-/-}$ → wt mice (89 ± 16 μg in wt → wt vs 59 ± 17 μg total iron in *Hfe*$^{-/-}$ → wt; $P < .005$) (Figure 4C). The opposite effect—an improved capacity to store iron in the spleen—developed in *Hfe*$^{-/-}$ mice reconstituted with wt cells (1711 ± 229 μg in *Hfe*$^{-/-}$ → *Hfe*$^{-/-}$ vs 4301 ± 702 μg iron/g dry weight in wt → *Hfe*$^{-/-}$ mice) (Figure 4B). We observed a 2-fold increase of total iron content in the spleens of wt → *Hfe*$^{-/-}$ mice (108 ± 24 μg total iron) compared with control *Hfe*$^{-/-}$ → *Hfe*$^{-/-}$ mice (49 ± 6 μg total iron; $P < .001$). These data indicate that

iron storage in the spleen is considerably altered in bone marrow chimeras of *Hfe* expression.

Augmented iron storage in the spleens of wt → $Hfe^{-/-}$ mice was accompanied by a decrease of approximately one third of total iron in the liver (621 ± 96 μg in wt → $Hfe^{-/-}$ vs 977 ± 135 μg total iron in $Hfe^{-/-}$ → $Hfe^{-/-}$; $P < .05$). Reductions in hepatic iron levels in wt → $Hfe^{-/-}$ mice started relatively early after BMT, and it reached statistical significance 6 weeks after BMT (data not shown). Based on calculations of total iron in the livers and spleens in 10-week-old $Hfe^{-/-}$ mice (Table 1), which totaled 565 ± 83 μg iron, 20-week-old $Hfe^{-/-}$ → $Hfe^{-/-}$ mice had gained, on average, an additional 461 μg excess iron (1026 ± 131 μg iron). In comparison, wt → $Hfe^{-/-}$ mice had gained only 296 μg iron (729 ± 98 μg iron; $P < .05$) in these organs. Our results indicate that iron absorption was partially inhibited in wt → $Hfe^{-/-}$ compared with $Hfe^{-/-}$ → $Hfe^{-/-}$ mice.

Contribution of *Hfe* gene–expressing macrophages to the regulation of hepatic hepcidin levels

Next, we evaluated the effect of BMT on the expression of the hepatic iron regulator hepcidin. $Hfe^{-/-}$ → $Hfe^{-/-}$ mice expressed 25% of hepcidin mRNA levels encountered in wt → wt mice ($P < .001$) (Figure 5). When $Hfe^{-/-}$ mice were reconstituted with wt bone marrow, hepcidin levels rose to 81% of those expressed in wt → wt mice ($P < .01$). Finally, wt mice reconstituted with *Hfe*-deficient bone marrow cells had a small decrease in hepcidin levels that did not reach statistical significance.

Discussion

Macrophages are central to the maintenance of iron homeostasis because they recycle iron from damaged and senescent red blood cells back into the circulation for reuse by erythropoiesis. In the present study, we explored the role of *Hfe* expression in macrophages in the maintenance of macrophage iron homeostasis and in the regulation of hepatic hepcidin production and iron loading. We showed that in murine hematopoietic-derived cells, *Hfe* is expressed predominantly in macrophages and Kupffer cells.

Using BMT, we effectively reconstituted wt mice with *Hfe*-deficient macrophages and $Hfe^{-/-}$ mice with wt macrophages. The donor phenotype was readily detected in the liver, duodenum, and spleen. Reconstitution in the spleen was highly efficient because 92% to 95% of *Hfe* mRNA was of donor origin. We found that BMT resulted in dramatic changes in the ability of splenic macrophages to store iron in *Hfe* chimeras. This was evidenced by diminished iron concentrations in the spleens of wt mice repopulated with *Hfe*-deficient marrow and, conversely, by the enhanced iron concentration found in the spleens of $Hfe^{-/-}$ mice reconstituted with wt marrow. Considerable evidence indicates that in HH, the lack of appropriately expressed HFE molecules leads to defective iron storage in macrophages and Kupffer cells.[43–45] In fact, a hallmark of the HH phenotype is the relative absence of iron in macrophages in spite of body iron overload. HH macrophages were found to have high iron regulatory protein (IRP) activity, which would prevent ferritin mRNA translation, the major cellular iron storage protein, and thus result in insufficient iron storage.[7] Convincingly, restoration of *HFE* expression in monocytes and monocytic cell lines that lack functional

HFE by means of transfection with wt *HFE* increases transferrin-dependent iron uptake[46] and inhibits iron efflux,[47] resulting in an augmentation of ferritin and cellular iron pools. These observations suggest that *HFE* mutations can directly affect iron accumulation in HH macrophages, independently of the presence of hepcidin. Our in vivo experiments on BMT chimeras demonstrate that *Hfe* expression in macrophages clearly determines the capacity of iron storage in the spleen. This could be attributed to a direct effect of *Hfe* expression in splenic macrophages and/or it can be a consequence of the elevation of hepatic hepcidin levels.

The second important consequence of *Hfe* deficiency is the higher setting of iron absorption levels in the duodenum. Considerable evidence now indicates that hepcidin plays a crucial role in the pathogenesis of HH and that the regulation of basal hepcidin levels is *Hfe* dependent. In fact, hepcidin levels are lower than expected in patients with HH[12] and in animal models,[10,11] particularly taking into account their body iron burden. How iron regulates hepatic hepcidin production remains to be elucidated. However, it is noteworthy that, though iron loading in mice strongly elicits the hepcidin response,[14] direct exposure of primary human hepatocyte cultures to iron does not lead to augmented hepcidin expression.[48] These observations indicate that hepcidin regulation by iron may rely on cross-communication between hepatocytes and RE macrophages in an Hfe-dependent fashion. Moreover, the fact that HH patients and animal models retain the capacity to appropriately regulate iron absorption in response to variations in iron status and erythroid demand[49,50] suggests that *Hfe* deficiency leads to quantitative rather than qualitative changes in hepcidin expression.

Our experiments, in which $Hfe^{-/-}$ mice were reconstituted with *Hfe*-expressing macrophages (wt → $Hfe^{-/-}$), show that restoring *Hfe* expression in RE cells can significantly inhibit iron loading. In fact, wt → $Hfe^{-/-}$ mice had hepatic iron levels that were approximately one third lower than those in $Hfe^{-/-}$ → $Hfe^{-/-}$ mice. This was observed in conjunction with a 3-fold increase in hepatic hepcidin levels in wt → $Hfe^{-/-}$ compared with $Hfe^{-/-}$ → $Hfe^{-/-}$ mice. These results may be underestimated because macrophages in the liver are replaced at a slower rate and less successfully than macrophages in hematopoietic tissues.[39,40] In fact, other studies using similar techniques estimated that donor bone marrow–derived cells repopulate only approximately 35% of liver macrophages within 14 weeks of BMT.[41] These values are close to those obtained in the present study using 2 different methods, GFP-marked macrophages and qRT-PCR to quantify donor-derived *Hfe* mRNA expression. Furthermore, BMT was performed when $Hfe^{-/-}$ mice were 6 weeks of age and when already significant excess iron had accumulated in their livers.

In previous experiments using the $B2m^{-/-}$ mouse, we found that adoptive transfer of wt fetal liver cells into lethally irradiated $B2m^{-/-}$ mice affected iron distribution in the liver in similar ways.[6] However, in these studies, no significant differences were detected in terms of liver iron loading and iron absorption between $B2m^{-/-}$ → $B2m^{-/-}$ and wt → $B2m^{-/-}$ mice. Several factors may explain these differences. First, unlike wt → $Hfe^{-/-}$ mice, not all cell lineages are reconstituted in wt → $B2m^{-/-}$ mice. For example, $CD8^+$ lymphocytes, which depend on interactions with MHC class 1 molecules on radioresistant cells in the thymus,[51] are not reconstituted in wt → $B2m^{-/-}$ mice (R.J.S., unpublished observations, September

2002, and Ohteki and MacDonald[52]). In turn, lymphocyte numbers have been shown to affect the degree of iron loading in animal models[18,53] and in patients with HH.[54,55] Second, *B2m*$^{-/-}$ mice also lack other MHC class 1 molecules, and recent studies indicate that other B2m-dependent MHC class 1 molecules may be involved in iron metabolism. For example, *HfeB2m*$^{-/-}$ compound mutants deposit more tissue iron than mice lacking Hfe only,[5] and mice lacking classic MHC class 1 molecules have higher hepatic iron levels than wt controls.[56] Overall, these studies indicate that there are important differences between the *Hfe*$^{-/-}$ and *B2m*$^{-/-}$ mouse models. Possibly other factors, including MHC class 1 molecules and lymphocytes, that may contribute to the pathogenesis of iron overload in *B2m*$^{-/-}$ mice remain unaffected by the adoptive transfer of hematopoietic cells. Third, the animals used in these studies were from different genetic backgrounds; *B2m*$^{-/-}$ mice were from the C57Bl/6 background and had a milder phenotype than *Hfe*$^{-/-}$ mice from the 129/SvEvTac background.

In reciprocal experiments in which wt mice were reconstituted with *Hfe*-deficient marrow, we found that liver iron content—and, hence, iron absorption levels—remained utterly unaffected. In fact, *Hfe*$^{-/-}$ → wt mice did not develop hemochromatosis, and hepcidin levels, albeit slightly decreased, did not reach statistical significance. Presumably, the remaining host Kupffer cells, expressing wt *Hfe*, were sufficient to maintain appropriate control of hepcidin and iron absorption levels. In fact, our experiments using GFP-marked BMCs showed that approximately 62% to 67% of hepatic F4/80^{+} macrophages remain GFP negative and are thus of host origin (Table 2).

Our interpretation is that *Hfe* expression by part of the Kupffer cells is sufficient to increase basal hepcidin production to such levels as to reduce duodenal iron absorption and, consequently, significantly inhibit iron loading in *Hfe*$^{-/-}$ mice and that it is enough to maintain appropriate iron homeostasis in wt mice. This suggests a central role for hepcidin rather than *Hfe* expression in the duodenum for the regulation of intestinal iron absorption and thus the control of iron loading. Supporting evidence for this interpretation is provided by studies on *Hfe*$^{-/-}$ mice crossed with transgenic mice overexpressing hepcidin under a liver-specific promoter demonstrating that constitutive hepcidin expression in the liver is sufficient to prevent iron accumulation normally observed in *Hfe*$^{-/-}$ mice.[57]

A clue to how hepcidin, in turn, may regulate iron absorption is provided by the recent finding that it can bind to Fp1, the major cellular iron exporter protein, inducing Fp1 internalization and degradation.[58] This presumably results in reduced iron efflux from hepatocytes, macrophages, and duodenal enterocytes.

In summary, our data show that the regulation of iron handling in macrophages is dependent on *Hfe* expression in these cells. They also show that *Hfe* expression by part of the Kupffer cells is sufficient to significantly increase basal hepcidin production in the liver and partially prevent iron loading in a background of total Hfe deficiency, and to maintain appropriate iron homeostasis in a wt background. This suggests an important contribution of *Hfe* expression in Kupffer cells to the regulation of hepatic hepcidin production.

Acknowledgments

We thank Christian Dallaire for his work with atomic absorption spectroscopy, Cristina Escrevente for her help with cell isolation, and Ovid Da Silva for his editorial assistance.

Supported by grant MOP44045 from the Canadian Institutes of Health Research (CIHR) and grant CBO/33485/99-00 from the Fundação para a Ciência e a Tecnologia. M.M.S. is the recipient of a CIHR New Investigator award.

References

1. Nichols GM, Bacon BR. Hereditary hemochromatosis: pathogenesis and clinical features of a common disease. Am J Gastroenterol. 1989; 84:851–862. [PubMed: 2667334]
2. Feder JN, Gnirke A, Thomas W, et al. A novel MHC class I-like gene is mutated in patients with hereditary haemochromatosis. Nat Genet. 1996; 13:399–408. [PubMed: 8696333]
3. Feder JN, Penny DM, Irrinki A, et al. The hemochromatosis gene product complexes with the transferrin receptor and lowers its affinity for ligand binding. Proc Natl Acad Sci U S A. 1998; 95:1472–1477. [PubMed: 9465039]
4. Zhou XY, Tomatsu S, Fleming RE, et al. HFE gene knockout produces mouse model of hereditary hemochromatosis. Proc Natl Acad Sci U S A. 1998; 95:2492–2497. [PubMed: 9482913]
5. Levy JE, Montross LK, Andrews NC. Genes that modify the hemochromatosis phenotype in mice. J Clin Invest. 2000; 105:1209–1216. [PubMed: 10791995]
6. Santos M, Schilham MW, Rademakers LH, Marx JJ, de Sousa M, Clevers H. Defective iron homeostasis in beta 2-microglobulin knockout mice recapitulates hereditary hemochromatosis in man. J Exp Med. 1996; 184:1975–1985. [PubMed: 8920884]
7. Cairo G, Recalcati S, Montosi G, Castrusini E, Conte D, Pietrangelo A. Inappropriately high iron regulatory protein activity in monocytes of patients with genetic hemochromatosis. Blood. 1997; 89:2546–2553. [PubMed: 9116301]
8. Knutson M, Wessling-Resnick M. Iron metabolism in the reticuloendothelial system. Crit Rev Biochem Mol Biol. 2003; 38:61–88. [PubMed: 12641343]
9. Bix M, Liao NS, Zijlstra M, Loring J, Jaenisch R, Raulet D. Rejection of class I MHC-deficient haemopoietic cells by irradiated MHC-matched mice. Nature. 1991; 349:329–331. [PubMed: 1987491]
10. Ahmad KA, Ahmann JR, Migas MC, et al. Decreased liver hepcidin expression in the Hfe knockout mouse. Blood Cells Mol Dis. 2002; 29:361–366. [PubMed: 12547226]
11. Muckenthaler M, Roy CN, Custodio AO, et al. Regulatory defects in liver and intestine implicate abnormal hepcidin and Cybrd1 expression in mouse hemochromatosis. Nat Genet. 2003; 34:102–107. [PubMed: 12704390]
12. Bridle KR, Frazer DM, Wilkins SJ, et al. Disrupted hepcidin regulation in HFE-associated haemochromatosis and the liver as a regulator of body iron homoeostasis. Lancet. 2003; 361:669–673. [PubMed: 12606179]
13. Park CH, Valore EV, Waring AJ, Ganz T. Hepcidin, a urinary antimicrobial peptide synthesized in the liver. J Biol Chem. 2001; 276:7806–7810. [PubMed: 11113131]
14. Pigeon C, Ilyin G, Courselaud B, et al. A new mouse liver-specific gene, encoding a protein homologous to human antimicrobial peptide hepcidin, is overexpressed during iron overload. J Biol Chem. 2001; 276:7811–7819. [PubMed: 11113132]
15. Nicolas G, Chauvet C, Viatte L, et al. The gene encoding the iron regulatory peptide hepcidin is regulated by anemia, hypoxia, and inflammation. J Clin Invest. 2002; 110:1037–1044. [PubMed: 12370282]
16. Nicolas G, Bennoun M, Devaux I, et al. Lack of hepcidin gene expression and severe tissue iron overload in upstream stimulatory factor 2 (USF2) knockout mice. Proc Natl Acad Sci U S A. 2001; 98:8780–8785. [PubMed: 11447267]
17. Nicolas G, Bennoun M, Porteu A, et al. Severe iron deficiency anemia in transgenic mice expressing liver hepcidin. Proc Natl Acad Sci U S A. 2002; 99:4596–4601. [PubMed: 11930010]

18. Miranda CJ, Makui H, Andrews NC, Santos MM. Contributions of beta2-microglobulin-dependent molecules and lymphocytes to iron regulation: insights from HfeRag1(−/−) and beta2mRag1(−/−) double knock-out mice. Blood. 2004; 103:2847–2849. [PubMed: 14656877]
19. Parkkila S, Waheed A, Britton RS, et al. Immunohistochemistry of HLA-H, the protein defective in patients with hereditary hemochromatosis, reveals unique pattern of expression in gastrointestinal tract. Proc Natl Acad Sci U S A. 1997; 94:2534–2539. [PubMed: 9122230]
20. Bastin JM, Jones M, O'Callaghan CA, Schimanski L, Mason DY, Townsend AR. Kupffer cell staining by an HFE-specific monoclonal antibody: implications for hereditary haemochromatosis. Br J Haematol. 1998; 103:931–941. [PubMed: 9886303]
21. Zhang AS, Xiong S, Tsukamoto H, Enns CA. Localization of iron metabolism-related mRNAs in rat liver indicate that HFE is expressed predominantly in hepatocytes. Blood. 2004; 103:1509–1514. [PubMed: 14563638]
22. Holmstrom P, Dzikaite V, Hultcrantz R, et al. Structure and liver cell expression pattern of the HFE gene in the rat. J Hepatol. 2003; 39:308–314. [PubMed: 12927914]
23. Hashimoto K, Hirai M, Kurosawa Y. Identification of a mouse homolog for the human hereditary haemochromatosis candidate gene. Biochem Biophys Res Commun. 1997; 230:35–39. [PubMed: 9020055]
24. Fleming RE, Holden CC, Tomatsu S, et al. Mouse strain differences determine severity of iron accumulation in Hfe knockout model of hereditary hemochromatosis. Proc Natl Acad Sci U S A. 2001; 98:2707–2711. [PubMed: 11226304]
25. Sproule TJ, Jazwinska EC, Britton RS, et al. Naturally variant autosomal and sex-linked loci determine the severity of iron overload in beta 2-microglobulin-deficient mice. Proc Natl Acad Sci U S A. 2001; 98:5170–5174. [PubMed: 11309500]
26. Dupic F, Fruchon S, Bensaid M, et al. Inactivation of the hemochromatosis gene differentially regulates duodenal expression of iron-related mRNAs between mouse strains. Gastroenterology. 2002; 122:745–751. [PubMed: 11875007]
27. Herrmann T, Muckenthaler M, van der Hoeven F, et al. Iron overload in adult Hfe-deficient mice independent of changes in the steady-state expression of the duodenal iron transporters DMT1 and Ireg1/ferroportin. J Mol Med. 2004; 82:39–48. [PubMed: 14618243]
28. Courselaud B, Troadec MB, Fruchon S, et al. Strain and gender modulate hepatic hepcidin 1 and 2 mRNA expression in mice. Blood Cells Mol Dis. 2004; 32:283–289. [PubMed: 15003819]
29. Levy JE, Montross LK, Cohen DE, Fleming MD, Andrews NC. The C282Y mutation causing hereditary hemochromatosis does not produce a null allele. Blood. 1999; 94:9–11. [PubMed: 10381492]
30. Petersen BE, Bowen WC, Patrene KD, et al. Bone marrow as a potential source of hepatic oval cells. Science. 1999; 284:1168–1170. [PubMed: 10325227]
31. Lagasse E, Connors H, Al-Dhalimy M, et al. Purified hematopoietic stem cells can differentiate into hepatocytes in vivo. Nat Med. 2000; 6:1229–1234. [PubMed: 11062533]
32. Takezawa R, Watanabe Y, Akaike T. Direct evidence of macrophage differentiation from bone marrow cells in the liver: a possible origin of Kupffer cells. J Biochem (Tokyo). 1995; 118:1175–1183. [PubMed: 8720132]
33. Okabe M, Ikawa M, Kominami K, Nakanishi T, Nishimune Y. 'Green mice' as a source of ubiquitous green cells. FEBS Lett. 1997; 407:313–319. [PubMed: 9175875]
34. Wang X, Montini E, Al-Dhalimy M, Lagasse E, Finegold M, Grompe M. Kinetics of liver repopulation after bone marrow transplantation. Am J Pathol. 2002; 161:565–574. [PubMed: 12163381]
35. Mallet VO, Mitchell C, Mezey E, et al. Bone marrow transplantation in mice leads to a minor population of hepatocytes that can be selectively amplified in vivo. Hepatology. 2002; 35:799–804. [PubMed: 11915025]
36. Wagers AJ, Sherwood RI, Christensen JL, Weissman IL. Little evidence for developmental plasticity of adult hematopoietic stem cells. Science. 2002; 297:2256–2259. [PubMed: 12215650]
37. Kanazawa Y, Verma IM. Little evidence of bone marrow-derived hepatocytes in the replacement of injured liver. Proc Natl Acad Sci U S A. 2003; 100:11850–11853. [PubMed: 12920184]

38. Fausto N. Liver regeneration and repair: hepatocytes, progenitor cells, and stem cells. Hepatology. 2004; 39:1477–1487. [PubMed: 15185286]
39. Krall WJ, Challita PM, Perlmutter LS, Skelton DC, Kohn DB. Cells expressing human glucocerebrosidase from a retroviral vector repopulate macrophages and central nervous system microglia after murine bone marrow transplantation. Blood. 1994; 83:2737–2748. [PubMed: 8167352]
40. Kennedy DW, Abkowitz JL. Kinetics of central nervous system microglial and macrophage engraftment: analysis using a transgenic bone marrow transplantation model. Blood. 1997; 90:986–993. [PubMed: 9242527]
41. Haghpassand M, Bourassa PA, Francone OL, Aiello RJ. Monocyte/macrophage expression of ABCA1 has minimal contribution to plasma HDL levels. J Clin Invest. 2001; 108:1315–1320. [PubMed: 11696576]
42. Nong Z, Gonzalez-Navarro H, Amar M, et al. Hepatic lipase expression in macrophages contributes to atherosclerosis in apoE-deficient and LCAT-transgenic mice. J Clin Invest. 2003; 112:367–378. [PubMed: 12897204]
43. Fillet G, Beguin Y, Baldelli L. Model of reticuloendothelial iron metabolism in humans: abnormal behavior in idiopathic hemochromatosis and in inflammation. Blood. 1989; 74:844–851. [PubMed: 2502204]
44. Flanagan PR, Lam D, Banerjee D, Valberg LS. Ferritin release by mononuclear cells in hereditary hemochromatosis. J Lab Clin Med. 1989; 113:145–150. [PubMed: 2783721]
45. Moura E, Noordermeer MA, Verhoeven N, Verheul AF, Marx JJ. Iron release from human monocytes after erythrophagocytosis in vitro: an investigation in normal subjects and hereditary hemochromatosis patients. Blood. 1998; 92:2511–2519. [PubMed: 9746792]
46. Montosi G, Paglia P, Garuti C, et al. Wild-type HFE protein normalizes transferrin iron accumulation in macrophages from subjects with hereditary hemochromatosis. Blood. 2000; 96:1125–1129. [PubMed: 10910932]
47. Drakesmith H, Sweetland E, Schimanski L, et al. The hemochromatosis protein HFE inhibits iron export from macrophages. Proc Natl Acad Sci U S A. 2002; 99:15602–15607. [PubMed: 12429850]
48. Nemeth E, Valore EV, Territo M, Schiller G, Lichtenstein A, Ganz T. Hepcidin, a putative mediator of anemia of inflammation, is a type II acute-phase protein. Blood. 2003; 101:2461–2463. [PubMed: 12433676]
49. Santos M, Clevers H, de Sousa M, Marx JJ. Adaptive response of iron absorption to anemia, increased erythropoiesis, iron deficiency, and iron loading in beta2-microglobulin knockout mice. Blood. 1998; 91:3059–3065. [PubMed: 9531620]
50. Ajioka RS, Levy JE, Andrews NC, Kushner JP. Regulation of iron absorption in Hfe mutant mice. Blood. 2002; 100:1465–1469. [PubMed: 12149232]
51. Werlen G, Hausmann B, Naeher D, Palmer E. Signaling life and death in the thymus: timing is everything. Science. 2003; 299:1859–1863. [PubMed: 12649474]
52. Ohteki T, MacDonald H. Major histocompatibility complex class I related molecules control the development of CD4+8− and CD4−8− subsets of natural killer 1.1+ T cell receptor-alpha/beta+ cells in the liver of mice. J Exp Med. 1994; 180:699–704. [PubMed: 8046344]
53. Santos MM, de Sousa M, Rademakers LH, Clevers H, Marx JJ, Schilham MW. Iron overload and heart fibrosis in mice deficient for both beta2-microglobulin and Rag1. Am J Pathol. 2000; 157:1883–1892. [PubMed: 11106561]
54. Cardoso EM, Hagen K, de Sousa M, Hultcrantz R. Hepatic damage in C282Y homozygotes relates to low numbers of CD8+ cells in the liver lobuli. Eur J Clin Invest. 2001; 31:45–53. [PubMed: 11168438]
55. Porto G, Vicente C, Teixeira MA, et al. Relative impact of HLA phenotype and CD4-CD8 ratios on the clinical expression of hemochromatosis. Hepatology. 1997; 25:397–402. [PubMed: 9021953]
56. Cardoso EM, Macedo MG, Rohrlich P, et al. Increased hepatic iron in mice lacking classical MHC class I molecules. Blood. 2002; 100:4239–4241. [PubMed: 12393413]
57. Nicolas G, Viatte L, Lou DQ, et al. Constitutive hepcidin expression prevents iron overload in a mouse model of hemochromatosis. Nat Genet. 2003; 34:97–101. [PubMed: 12704388]

58. Nemeth E, Tuttle MS, Powelson J, et al. Hepcidin regulates iron efflux by binding to ferroportin and inducing its internalization. Science. 2004; 306:2090–2093. [PubMed: 15514116]

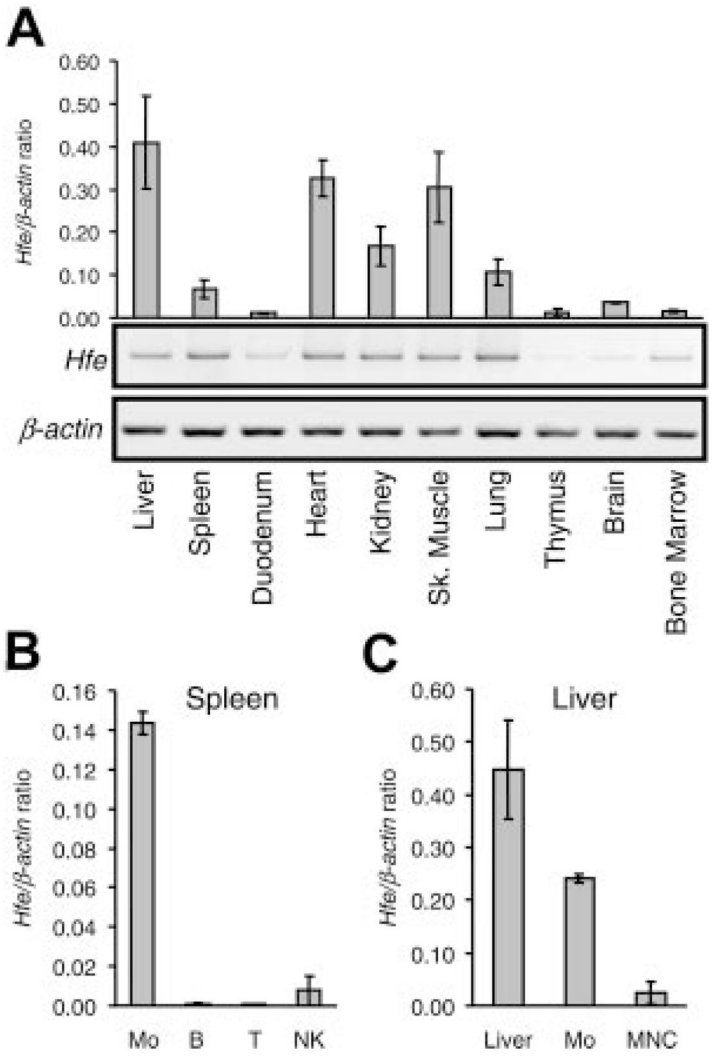

Figure 1. Analysis of Hfe gene expression

Hfe expression was analyzed in various organs and in isolated cell fractions from spleen and liver. (A) mRNA was isolated from various organs, as indicated, and was used to synthesize cDNA. *Hfe* mRNA expression was quantified by qRT-PCR and normalized to Actb (graph). The *Hfe/Actb* × 10^3 ratio is shown. Conventional RT-PCR products were visualized by ethidium bromide staining in 1.0% agarose gels. (B) *Hfe* mRNA expression in positively selected splenic macrophages (Mo), B lymphocytes (B), T lymphocytes (T), NK cells, and (C) whole liver (liver), liver macrophages (Mo), and mononuclear cells (MNC) assessed by qRT-PCR and normalized to Actb. The *Hfe/Actb* × 10^3 ratio is shown. Results are presented as mean ± SD (n = 3 mice per organ or cell isolate).

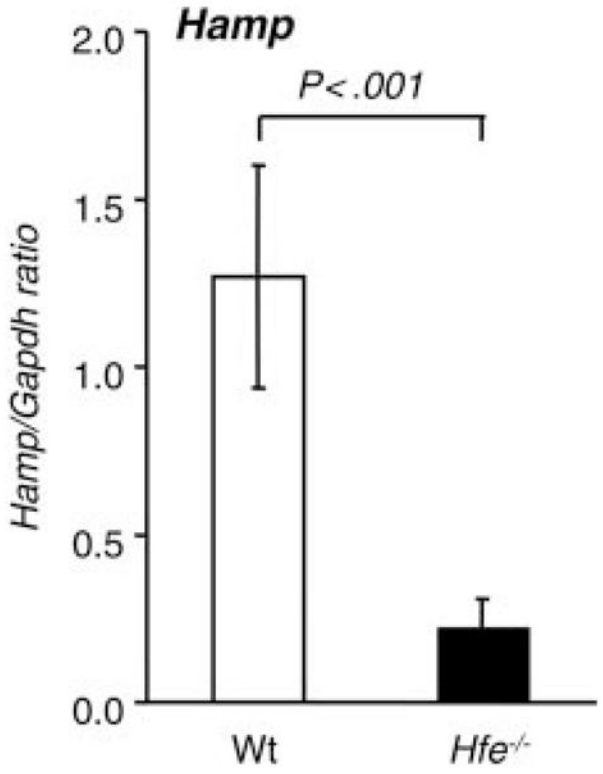

Figure 2. Hepatic hepcidin expression in 10-week-old *Hfe*$^{-/-}$ mice from the 129/SvEvTac background

Hamp mRNA expression was quantified by qRT-PCR and normalized to *Gapdh*. The *Hamp/Gapdh* ratio is shown. Results are presented as mean ± SD (n = 6 mice per group). Statistical analysis was performed by Student *t* test.

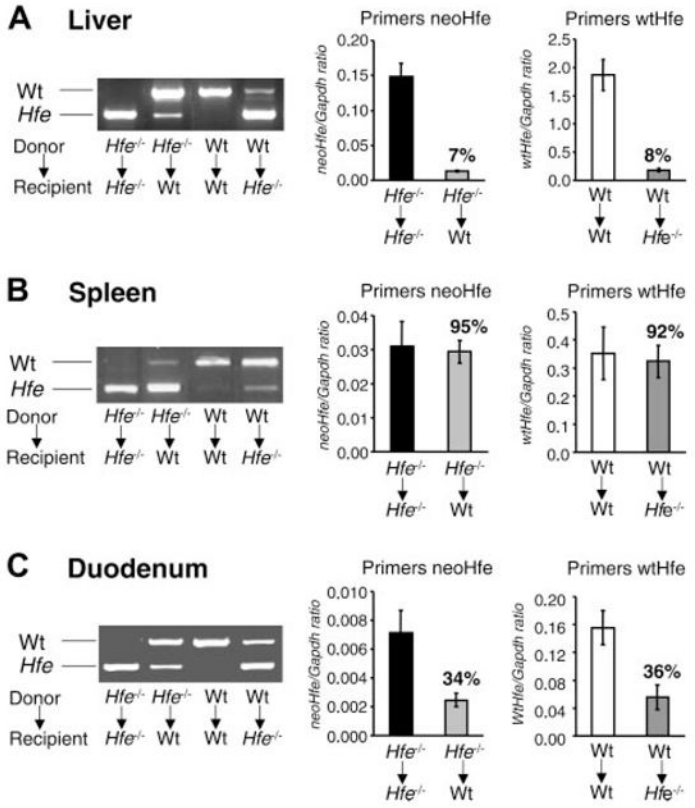

Figure 3. Engraftment of bone marrow–derived cells in the liver, spleen, and duodenum

Total RNA was isolated from the (A) liver, (B) spleen, and (C) duodenum 14 weeks after BMT and was used to synthesize cDNA. (left) cDNA was PCR amplified with one set of primers spanning exons 3 and 6 of the mouse *Hfe* gene (primers *Hfe*) and the products were visualized by ethidium bromide staining in 1.0% agarose gels. In $Hfe^{-/-} \rightarrow$ wt mice, but not in wt $\rightarrow$ wt mice, the amplification product of donor $Hfe^{-/-}$ mice (*Hfe,* 499 bp) appears in wt recipient mice (wt, 775 bp) after transplantation. Conversely, in wt $\rightarrow$ $Hfe^{-/-}$ mice, but not in $Hfe^{-/-} \rightarrow Hfe^{-/-}$ mice, the amplification product of donor wt mice (wt, 775 bp) appears in $Hfe^{-/-}$ recipient mice (*Hfe,* 499 bp) after transplantation. One representative mouse is shown per BMT group. (right) Quantification of donor *Hfe* mRNA by qRT-PCR and normalized to *Gapdh.* Two distinct sets of primers were used—*neoHfe* and *wtHfe*—shown separately in the graphs. *neoHfe/Gapdh* × 10^3 and *wtHfe/Gapdh* × 10^3 ratios are presented. Results are mean ± SD (n = 6–12 mice per group).

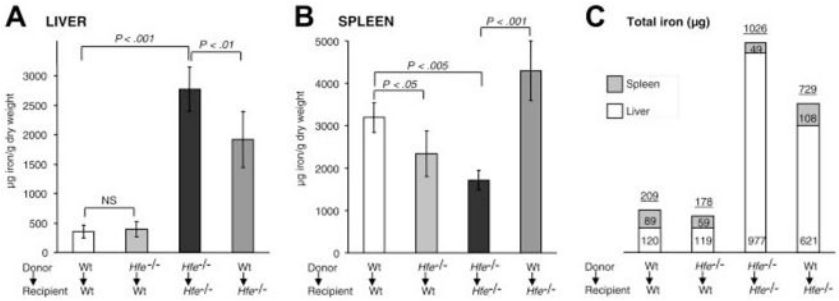

Figure 4. Liver and spleen iron storage in mice 14 weeks after BMT

Iron concentration in the (A) liver and (B) spleen. Results are presented as mean ± SD (n = 6–12). Statistical analysis was performed by one-way ANOVA. (C) Relative amounts of total iron stored in the liver and spleen. Each rectangle represents the absolute proportion of iron, expressed in micrograms, found in the liver (☐) and spleen (▨). Numbers on top of the boxes indicate cumulative iron in the liver and spleen.

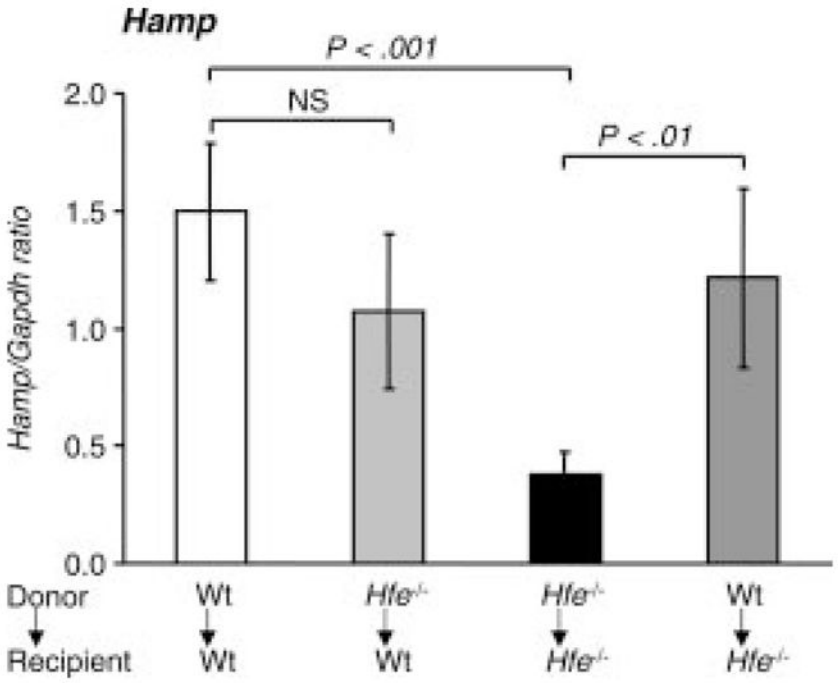

Figure 5. Hepcidin levels in mice 14 weeks after BMT

Quantitative alterations in liver hepcidin *(Hamp)* mRNA levels were measured by qRT-PCR and normalized to *Gapdh*. The *Hamp/Gapdh* ratio is shown. Results are presented as mean ± SD (n = 6–12). Statistical analysis was performed by one-way ANOVA.

Table 1

Iron parameters in 129/SvEvTac *Hfe*$^{-/-}$ mice

Parameter	WT	*Hfe*$^{-/-}$	*P*
Serum iron, μM	32 ± 7	44 ± 5	< .01
Transferrin saturation, %	57 ± 4	110 ± 12	< .001
Iron concentration, μg iron/g dry weight			
Liver	322 ± 50	1675 ± 249	< .001
Spleen	2451 ± 671	1791 ± 257	NS

Data are presented as mean ± SD.

NS indicates not significant.

Table 2

Degree of engraftment of donor macrophages in the livers of recipient mice after BMT

Donor → recipient	n	$GFP^+F4/80^+$ donor macrophages, %	$GFP^-F4/80^+$ host macrophages, %
GFP^+wt → wt	4	35 ± 3	65 ± 3
GFP^+*Hfe*$^{-/-}$ → wt	4	37 ± 2	63 ± 2
GFP^+*Hfe*$^{-/-}$ → *Hfe*$^{-/-}$	4	33 ± 3	67 ± 3
GFP^+wt → *Hfe*$^{-/-}$	4	36 ± 4	64 ± 4

Liver NPC fractions from mice that underwent BMT were analyzed by flow cytometry for the presence of GFP^+ donor-derived macrophages. NPCs were stained for the macrophage marker F4/80, and the percentage of GFP^+ and GFP^- within all $F4/80^+$ cells is shown. Data are presented as mean ± SD.